

**Computing the effective Hamiltonian of low-energy vacuum gauge fields**R. Millo<sup>1,2,\*</sup> and P. Faccioli<sup>1,2</sup><sup>1</sup>*Università degli Studi di Trento, Via Sommarive 14, Povo (Trento), Italy*<sup>2</sup>*INFN, Gruppo Collegato di Trento, Via Sommarive 14, Povo (Trento), Italy*

(Received 20 May 2011; published 23 August 2011)

A standard approach to investigate the nonperturbative QCD dynamics is through vacuum models which emphasize the role played by specific gauge field fluctuations, such as instantons, monopoles, or vortices. The effective Hamiltonian describing the dynamics of the low-energy degrees of freedom in such approaches is usually postulated phenomenologically, or obtained through uncontrolled approximations. In a recent paper, we have shown how lattice field theory simulations can be used to rigorously compute the effective Hamiltonian of arbitrary vacuum models by stochastically performing the path integral over all the vacuum field fluctuations which are not explicitly taken into account. In this work, we present the first illustrative application of such an approach to a gauge theory and we use it to compute the instanton size distribution in  $SU(2)$  gluon dynamics in a fully model independent and parameter-free way.

DOI: [10.1103/PhysRevD.84.034504](https://doi.org/10.1103/PhysRevD.84.034504)

PACS numbers: 12.38.Gc, 12.38.-t

**I. INTRODUCTION**

Contemporary lattice gauge theory (LGT) simulations allow one to compute from first principles a large class of hadronic matrix elements in QCD, in some cases even within a few percent accuracy. On the other hand, such simulations do not provide much detailed information about the structure of the gluonic fluctuations which drive the QCD dynamics in the strongly coupled regime. For example, despite several decades of investigations, the dynamical processes underlying chiral symmetry breaking and color confinement are still a matter of debate.

The problem of identifying the dynamical origin of such nonperturbative phenomena has been extensively addressed in the context of phenomenological models which emphasize the role played by specific vacuum field fluctuations, such as e.g. instantons [1], monopoles [2], and center vortices [3]. The configuration space of these models is defined by the collective coordinates of the selected low-energy vacuum fields. On the other hand, the statistical distribution of such collective coordinates (or, equivalently, their effective Hamiltonian) is usually obtained through approximations upon which one does not have full theoretical control, e.g. by completely neglecting the contribution of the fluctuations around the chosen vacuum fields [4] or by estimating the role of such fluctuations through variational methods [5].

In principle, LGT simulations can be used to test the predictions of the phenomenological vacuum models, for example, by looking for some specific signatures of the dynamics generated by instantons [6,7], monopoles [8], or vortices [9]. On the other hand, the model dependence

associated to the effective Hamiltonian for the vacuum field degrees of freedom makes it difficult to draw definitive conclusions about the validity of a given model. Indeed, a moderate disagreement with the experimental data or with the results of lattice QCD simulations may be due to either a wrong choice of the low-energy vacuum fields, or to the strong approximations involved in the definition of their partition function.

In order to tackle this problem, in a recent work we have developed a technique, which we shall refer to as vacuum manifold projection (VMP), by which lattice simulations are used to rigorously compute the effective Hamiltonian of arbitrary vacuum models [10], in a model independent way. This is done by nonperturbatively performing the path integral over all the vacuum field configurations which are not explicitly taken into account in the given low-energy vacuum model. For example, in an instanton model, one performs the path integral over all the configurations which are orthogonal to the functional manifold spanned by multi-instanton configurations. Clearly, once the partition function has been evaluated from first principles, any failure of the model must be entirely due to the wrong choice of the effective low-energy degrees of freedom.

In our first work, the VMP method was illustrated and tested by evaluating the instanton-anti-instanton interaction in a simple quantum-mechanical toy model [10]. Here, we present the first application to a gauge theory. In particular, we use the VMP method to compute the instanton size distribution in two-color Yang-Mills theory.

The paper is organized as follows. In Sec. II we review the VMP method for a generic choice of vacuum field degrees of freedom. In Sec. III we focus on an effective theory based on instanton degrees of freedom and we use the VMP method to compute the instanton size distribution in  $SU(2)$  gluon dynamics. The main results, conclusions, and perspectives are summarized in Sec. IV.

\*Present address: Theoretical Physics Division, Department of Mathematical Sciences, University of Liverpool, Liverpool, L69 3BX, UK.

## II. THE VACUUM MANIFOLD PROJECTION METHOD

Let us consider a gauge theory defined by the (Euclidean) path integral

$$Z = \int \mathcal{D}A_\mu e^{-S[A_\mu]}, \quad (1)$$

where the  $S[A_\mu]$  formally includes the gauge-fixing and ghost terms, along with the fermionic determinant. In the following, we shall assume that the path integral is defined in the Landau gauge, although in principle the formalism to be presented here holds in any fixed gauge.

Let  $\gamma \equiv (\gamma_1, \dots, \gamma_k)$  be a set of  $k$  collective coordinates which parametrize a manifold  $\mathcal{M}$  of vacuum field configurations  $\tilde{A}_\mu(x; \gamma_1, \dots, \gamma_k)$ . For example, in instanton models,  $\gamma_1, \dots, \gamma_N$  are the positions, sizes, and color orientations of all the pseudoparticles in the instanton ensemble. However, in general, we do *not* require the field configurations  $\tilde{A}_\mu(x; \gamma_1, \dots, \gamma_k)$  to be solutions of the classical Yang-Mills equations of motion.

For any given choice of the set of collective coordinates  $\gamma$ , a generic vacuum gauge field configuration  $A_\mu(x)$  contributing to the path integral (1) can be decomposed as

$$A_\mu(x) \equiv \tilde{A}_\mu(x; \gamma_1, \dots, \gamma_k) + B_\mu(x), \quad (2)$$

where  $B_\mu(x)$  will be referred to as the ‘‘fluctuation field.’’ Our goal is to use LGT to perform the path integral over such a field. More precisely, we want to compute the function  $\mathcal{H}(\gamma_1, \dots, \gamma_k)$  such that

$$Z = \int \mathcal{D}A_\mu e^{-S[A_\mu]} = \int d\gamma_1 \dots d\gamma_k e^{-\mathcal{H}(\gamma_1, \dots, \gamma_k)}. \quad (3)$$

Equation (3) defines a statistical model in which  $\gamma_1, \dots, \gamma_k$  are the effective low-energy degrees of freedom and  $\mathcal{H}(\gamma_1, \dots, \gamma_k)$  is the effective Hamiltonian. We shall see shortly that such function is defined as the logarithm of a gauge-fixed path integral.

Since the representation (3) of the path integral contains  $k$  additional integrals over  $d\gamma_1, \dots, d\gamma_k$ , we need to introduce  $k$  constraints. A natural choice is to impose a set of  $k$  orthogonality conditions:

$$(B_\mu(x), g_{\gamma_i, \mu}(x, \bar{\gamma})) \equiv \text{Tr}_c \left\{ \int d^4x B_\mu(x) g_{\gamma_i, \mu}(x, \bar{\gamma}) \right\} = 0, \quad (4)$$

$$i = 1, \dots, k$$

$$g_{\gamma_i, \mu}(x, \bar{\gamma}) = \left. \frac{\partial}{\partial \gamma_i} \tilde{A}_\mu(x; \gamma) \right|_{\gamma = \bar{\gamma}}. \quad (5)$$

We observe that the functions  $\{g_{\gamma_i}(x, \bar{\gamma})\}_{i=1, \dots, k}$  identify the  $k$  directions tangent to the manifold  $\mathcal{M}$  of background vacuum fields, in the point of curvilinear coordinates  $\bar{\gamma} = (\bar{\gamma}_1, \dots, \bar{\gamma}_k)$ —see Fig. 1. We consider only choices

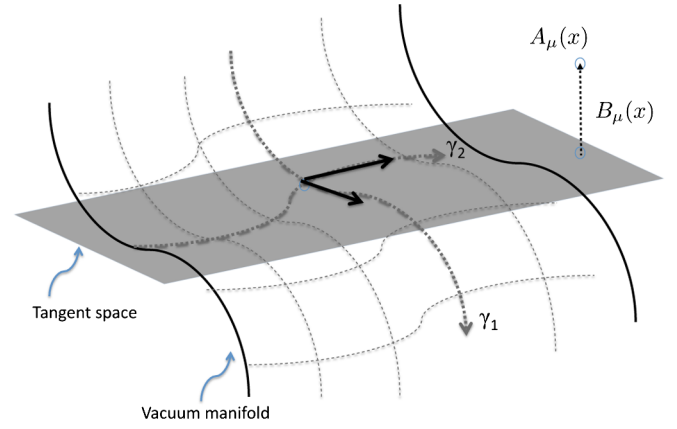


FIG. 1 (color online). Pictorial representation of the projection of the gauge field configuration  $A_\mu(x)$  of the path integral  $Z = \int \mathcal{D}A_\mu e^{-S[A_\mu]}$  onto a specific vacuum field manifold, spanned by two collective coordinates  $\gamma_1$ , and  $\gamma_2$ . A generic path is represented by a point in this three-dimensional space. The constraints given in Eq. (4) imply that the fluctuation field  $B_\mu(x)$  is perpendicular to the plane tangent to the manifold in a given point.

of the manifold  $\mathcal{M}$  and of the point  $\bar{\gamma}$  such that the vectors (5) define a system of coordinates.

In the path-integral formalism, the orthogonality conditions (4) can be implemented by introducing a Fadeev-Popov representation of the unity. After some formal manipulation (see e.g. Refs. [5,10]), one arrives at an expression in the form of Eq. (3), where the effective Hamiltonian  $\mathcal{H}(\gamma_1, \dots, \gamma_k)$  is defined as

$$\mathcal{H}(\gamma_1, \dots, \gamma_k) = -\log \left\{ \int \mathcal{D}B \delta[\partial_\mu B_\mu] \times \prod_i \delta[(B_\mu(x), g_{\gamma_i, \mu}(x, \bar{\gamma}))] \times \Phi[\tilde{A}(x, \gamma) + B(x)] e^{-S[\tilde{A}(x, \gamma) + B(x)]} \right\}, \quad (6)$$

where  $\Phi$  is a Jacobian factor and reads

$$\Phi^{-1}[A_\mu(x)] = \int \prod_{l=1}^k d\gamma_l \int \mathcal{D}U^\Omega \delta[\partial_\mu A_\mu^\Omega] \times \prod_i \delta[(A_\mu^\Omega(x) - \tilde{A}_\mu(x, \gamma), g_{\gamma_i, \mu}(x, \bar{\gamma}))]. \quad (7)$$

$U^\Omega(x)$  denotes a generic gauge transformation and  $A_\mu^\Omega(x)$  is result of gauge transforming the field  $A_\mu(x)$  according to  $U^\Omega(x)$ . Note that, while the path integral  $Z$  is obviously gauge invariant, the definition of the effective Hamiltonian  $\mathcal{H}(\gamma_1, \dots, \gamma_k)$  relies on the choice of the gauge, in this case the Landau gauge.

The orthogonality condition (4) and the system of coordinates (5) can be used to devise an algorithm to explicitly compute the effective Hamiltonian (6). We begin by observing that, on such a system of coordinates, a functional

point  $A_\mu(x)$  which belongs to the vacuum field manifold  $\mathcal{M}$  is identified by the coordinates  $(\Psi_1, \dots, \Psi_k)$  with

$$\Psi_i[A_\mu(x)] = (A_\mu(x), g_{\gamma_i, \mu}(x, \bar{\gamma})). \quad (8)$$

Clearly, also field configurations which lie in a functional neighborhood of the manifold  $\mathcal{M}$  can be projected onto the same system of coordinates. In this case, for an arbitrary fixed choice of  $\bar{\gamma}$ , the orthogonality conditions (4) imply that there exists a set of collective coordinates  $\gamma$  such that

$$\begin{aligned} \Psi_i[A_\mu(x)] &\equiv (A_\mu(x), g_{\gamma_i, \mu}(x, \bar{\gamma})) \\ &= (\tilde{A}_\mu(x; \gamma) + B_\mu(x), g_{\gamma_i, \mu}(x, \bar{\gamma})) \\ &= (\tilde{A}_\mu(x; \gamma), g_{\gamma_i, \mu}(x, \bar{\gamma})), \\ (i &= 1, \dots, k). \end{aligned} \quad (9)$$

Such an equation allows one to associate a set of collective coordinate  $\gamma = (\gamma_1, \dots, \gamma_k)$  to any Landau gauge-fixed gluon field configuration  $A_\mu(x)$  which lies in the functional vicinity of the manifold  $\mathcal{M}$ . Based on this result, it is immediate to devise an algorithm to evaluate the path integral  $\mathcal{H}(\gamma_1, \dots, \gamma_k)$  stochastically, from LGT simulations:

- (1) An ensemble of  $N_{\text{conf}}$  independent lattice configurations  $\{U_\mu^{(1)}(x), \dots, U_\mu^{(N_{\text{conf}})}(x)\}$  is generated by standard LGT simulations.
- (2) From such configurations, an ensemble of Landau *gauge-fixed* lattice configurations  $\{U_\mu^{g(1)}(x), \dots, U_\mu^{g(N_{\text{conf}})}(x)\}$  is obtained, e.g. using the procedure illustrated in Refs. [11,12].
- (3) From each lattice configuration, the gluon field  $A_\mu^g(x)$  at each lattice site is calculated from the gauge-fixed lattice link variables  $U_\mu^g(x)$ , for example using the discretized definition

$$A_\mu^g(x) = \frac{1}{2ai} (U_\mu^g(x) - U_\mu^g(x)^\dagger). \quad (10)$$

- (4)  $k$  nonlinear equations for the  $\gamma_1, \dots, \gamma_k$  variables are obtained from Eq. (9):

$$\begin{aligned} (A_\mu^g(x), g_{\gamma_1, \mu}^g(x, \bar{\gamma})) &= (\tilde{A}_\mu^g(x, \gamma), g_{\gamma_1, \mu}^g(x, \bar{\gamma})) \\ &\quad \dots \\ (A_\mu^g(x), g_{\gamma_k, \mu}^g(x, \bar{\gamma})) &= (\tilde{A}_\mu^g(x, \gamma), g_{\gamma_k, \mu}^g(x, \bar{\gamma})). \end{aligned} \quad (11)$$

On the lattice, the inner products above are obviously represented as discretized sums,

$$\begin{aligned} (A_\mu^g(x), g_{\gamma_i, \mu}^g(x, \bar{\gamma})) &= a^4 \sum_n \text{Tr}_C [A_\mu^g(n) g_{\gamma_i}^g(n; \bar{\gamma})], \\ (i &= 1, \dots, k), \end{aligned} \quad (12)$$

where  $n$  runs over all the lattice sites and  $\text{Tr}_C$  refers to the trace over color labels.

Notice that the quantities on the left-hand side of Eq. (11) are  $c$  numbers which depend only on the lattice configuration and on the projection point  $\bar{\gamma}$ . They correspond to the components of the lattice

field  $A_\mu^g(x)$  in the system of coordinates defined by the tangent vectors  $g_{\gamma_i, \mu}^g(x, \bar{\gamma})$ .

On the other hand, the quantities on the right-hand side of Eq. (11) are functions of the curvilinear coordinates  $\gamma$  which do not depend on the lattice configurations  $A_\mu^g(x)$ . These functions are completely specified, for any given fixed choice of the vacuum field manifold  $\mathcal{M}$  and of the projection point  $\bar{\gamma}$ .

Hence, for any lattice configuration  $U_\mu^g(x)$  the set of equations (11) can be numerically solved for  $\gamma = (\gamma_1, \dots, \gamma_k)$ .

- (5) The frequency histogram of  $\gamma_1, \dots, \gamma_k$  obtained by repeating this procedure for a large number  $N_{\text{conf}}$  of statistically independent lattice gauge field configurations represents the probability  $\mathcal{P}(\gamma_1, \dots, \gamma_k)$  of a given set of curvilinear coordinates. Then the effective Hamiltonian for  $\gamma_1, \dots, \gamma_k$  is obviously given by

$$\mathcal{H}(\gamma_1, \dots, \gamma_k) = -\log \mathcal{P}(\gamma_1, \dots, \gamma_k). \quad (13)$$

Some comments on the VMP algorithm are in order. First of all, we emphasize that such a scheme relies on the assumption that the background field configurations  $\tilde{A}_\mu(x; \gamma)$  are the relevant vacuum degrees of freedom. More precisely, we are requiring that the field configurations which contribute the most to the path integral (1) lie in some functional neighborhood of the manifold  $\mathcal{M}$ , so that they can be projected onto the system of coordinates defined in Eq. (5). Under such a condition, the definition of the effective Hamiltonian  $\mathcal{H}(\gamma_1, \dots, \gamma_k)$  is unique and does not depend on any additional external parameters.

Once the effective Hamiltonian has been determined, arbitrary vacuum-to-vacuum matrix elements can be approximately computed by neglecting the contribution of the fluctuation field  $B_\mu(x)$  to the operators. For example, if  $\hat{O}(x)$  is a local operator which depends on the gluonic field  $A_\mu(x)$ , one has

$$\begin{aligned} \langle 0 | \hat{O}[A_\mu(x)] | 0 \rangle &= \frac{1}{Z} \int \mathcal{D}A_\mu O[A_\mu(x)] e^{-S[A_\mu]} \\ &\simeq \frac{1}{Z} \int d\gamma_1 \dots d\gamma_k O[\tilde{A}_\mu(x; \gamma)] e^{-\mathcal{H}(\gamma_1, \dots, \gamma_k)}. \end{aligned} \quad (14)$$

Since the effective Hamiltonian is evaluated from first principles, any violation of this identity implies that the fluctuation field  $B_\mu$  plays an important role in the observable associated to these matrix elements or that there are important fluctuations in the path integral which are very far from the functional manifold  $\mathcal{M}$ , hence cannot be projected onto the system of coordinates (5). In both cases, this would represent an unambiguous signature of the failure of the vacuum field model.

We also stress that the VMP results do not depend on the choice of the gauge. Indeed, in Ref. [10] it was shown that once the system of Eq. (11) is satisfied in one gauge, it holds also in any other gauge.

Finally, we note that the VMP procedure is conceptually analog to a technique routinely adopted in classical statistical mechanics to evaluate the potential of mean force  $G(\gamma_1, \dots, \gamma_k)$  as a function of a set of collective coordinates  $\gamma_1, \dots, \gamma_k$  (see e.g. [13] and references therein). In the canonical ensemble, the potential of mean-force (free energy) is defined as

$$e^{-\beta G(\gamma_1, \dots, \gamma_k)} = \int d\Gamma \prod_{i=1}^k \delta[\gamma_i - f_i(\Gamma)] e^{-\beta H(\Gamma)} \quad (\beta = 1/k_B T), \quad (15)$$

where  $\Gamma$  is the phase-space variable,  $H(\Gamma)$  is the Hamiltonian, and the functions  $f_i(\Gamma)$  specify the definition of the macroscopic collective coordinate  $\gamma_i$  in terms of the microscopic phase-space variable  $\Gamma$ . The system's partition function reads

$$Z = \int d\gamma_1 \dots d\gamma_k e^{-\beta G(\gamma_1, \dots, \gamma_k)}, \quad (16)$$

in complete analogy with Eq. (3). In order to evaluate  $G(\gamma_1, \dots, \gamma_k)$ , one generates an ensemble of statistically independent equilibrium configurations  $\{\Gamma_1, \dots, \Gamma_{N_{\text{conf}}}\}$ , by means of Monte Carlo or molecular dynamics simulations, and evaluates  $\gamma_1, \dots, \gamma_k$  from  $\gamma_i = f_i(\Gamma)$ , for each of such configurations. In the limit of large number of equilibrium configurations  $N_{\text{conf}}$ , the frequency histogram for the values  $\gamma_1, \dots, \gamma_k$  obtained this way yields the equilibrium probability function for the collective coordinates,  $\mathcal{P}(\gamma_1, \dots, \gamma_k)$ . The negative of the logarithm of such a probability defines by construction the free energy

$$-\beta G(\gamma_1, \dots, \gamma_k) = \log \mathcal{P}(\gamma_1, \dots, \gamma_k). \quad (17)$$

### III. CALCULATION OF THE INSTANTON SIZE DISTRIBUTION IN $SU(2)$ GLUON DYNAMICS

As a first illustrative application of the VMP method, in this section we specialize on the case in which the gauge theory is  $SU(2)$  gluon dynamics and the vacuum manifold  $\mathcal{M}$  is constructed by superimposing singular-gauge instanton and anti-instanton configurations, i.e. in the so-called instanton vacuum.

Instanton vacuum models have been successfully used to investigate the dynamics of light hadrons [1] and the breaking of chiral symmetry [14] in QCD. It has been shown that this model is able to reproduce the spectrum of the observed lowest-lying hadrons [15–17] and of scalar and pseudoscalar glueballs [18–21], along with the electromagnetic structure of pions and nucleons [22–25]. In addition, the instanton liquid model provides an explanation of the  $\Delta I = 1/2$  rule for nonleptonic hadron decays of kaons [26]

and hyperons [27], by promoting nonperturbative scalar diquark correlations [28]. While it is well known that semiclassically inspired vacuum models based only on singular-gauge instantons do not provide color confinement, a finite string tension was obtained in models employing cocktails of regular- and singular-gauge instantons and merons [4,29].

From the theoretical point of view, a main limitation of the instanton approach to QCD resides in the well-known “infrared catastrophe” of the semiclassical dilute instanton gas approximation: in the presence of quantum fluctuations, isolated instantons tend to swell. The instanton liquid model originates from the observation that such an infrared divergence can be cured if correlations between pseudoparticles are included [5,30]. Unfortunately, allowing for such interactions implies giving up a rigorous semiclassical theory of the QCD vacuum. In the so-called instanton liquid models, the size distribution of the pseudoparticles is estimated using variational or phenomenological arguments. In such approaches, the typical instanton size in QCD is found to be of the order of  $1/3$  fm—see e.g. [1,5].

In order to extract information about the structure of instanton ensemble directly from LGT simulations, algorithms such as cooling [31] or eigenvalue filtering [7] have been proposed. Such methods provide techniques to filter out (not integrate out) the high-frequency quantum content of lattice configurations. A problem with these methods is that their results critically depend on the choice of additional uncontrolled parameters, such as the number of cooling steps or of the number of retained low-lying eigenmodes of the Dirac operator. Clearly, such a dependence introduces some degree of arbitrariness in the results. For example, the instanton density vanishes in the limit of a very large number of cooling steps.

The goal of this section is to show that the VMP method can be used to rigorously evaluate the instanton size distribution directly from lattice simulations, without introducing any arbitrary parameter. The choice of focusing on  $SU(2)$  Yang-Mills theory was made in order to keep the analytical and numerical calculations as simple as possible.

#### A. The instanton vacuum manifold

We begin our calculation by defining the manifold of vacuum field configurations. In two-color Yang-Mills theory, the classical field of an individual instanton or anti-instanton is specified by four collective coordinates:  $\gamma = (z, \rho, \theta_1, \theta_2, \theta_3)$ , where  $z$  is the position of the pseudoparticle,  $\rho$  is its size, and  $\theta_i$  ( $i = 1, 2, 3$ ) are three angles which specify a  $SU(2)$  matrix in color space according to

$$U = \exp(i\theta_k \tau_k). \quad (18)$$

A configuration of  $N_+$  instanton and  $N_-$  instantons  $A_\mu(x; \gamma_1, \dots, \gamma_{N_+ + N_-})$  can be constructed in the so-called sum *ansatz*, i.e. by superposing the classical fields of the pseudoparticles:

$$\tilde{A}_\mu(x; \gamma) = \sum_{i=1}^{N_+ + N_-} \tilde{A}_\mu^i(x; \gamma_i), \quad (19)$$

where  $\tilde{A}_\mu^i(x; \gamma_i)$  is the classical field of the  $i$ th pseudoparticle:

$$\tilde{A}_\mu^i(x; \gamma_i) = U^i \tau^a U^{\dagger, i} \bar{\eta}^a_{\mu\nu} \frac{\rho_i^2}{(x - z^i)^2} \frac{(x - z^i)_\nu}{(x - z^i)^2 + \rho_i^2},$$

(for instantons) (20)

$$\tilde{A}_\mu^i(x; \gamma_i) = U^i \tau^a U^{\dagger, i} \eta^a_{\mu\nu} \frac{\rho_i^2}{(x - z^i)^2} \frac{(x - z^i)_\nu}{(x - z^i)^2 + \rho_i^2},$$

(for anti-instantons). (21)

$\bar{\eta}^a_{\mu\nu}$  and  $\eta^a_{\mu\nu}$  are the so-called 't Hooft indexes. It is important to emphasize that the field obtained from the sum ansatz (19) is not in general a solution of the Euclidean Yang-Mills equation of motion.

An effective theory for the two-color Yang-Mills (YM) theory can be obtained if the path integral over all the gauge field configurations is replaced by the sum over all the configurations of a grand-canonical statistical ensemble of singular-gauge instantons and anti-instantons:

$$Z_{\text{YM}} = \sum_{N_+, N_-} \frac{1}{N_+! N_-!} e^{i\theta(N_+ - N_-)} \int \prod_i^{N_+ + N_-} d\gamma_i e^{-\mathcal{H}(\gamma_1, \dots, \gamma_N)},$$

(22)

where  $\theta$  is the angle associated to strong CP violation and  $\mathcal{H}(\gamma_1, \dots, \gamma_N)$  is the effective Hamiltonian, which represents the functional integral over the configurations which do not belong to the instanton vacuum manifold. In the analogy with classical statistical mechanics discussed in Sec. II, this term can be interpreted as the ‘‘potential of mean force’’ between the pseudoparticles generated by all other quantum gauge field fluctuations in the path integral. Clearly, if the effective Hamiltonian  $\mathcal{H}(\gamma_1, \dots, \gamma_N)$  is calculated nonperturbatively from first principles, then Eq. (22) provides an exact representation of the path integral, which does not rely at all on the semiclassical approximation.

If the instanton ensemble is not too dense, it is possible to perform a many-body expansion of the effective Hamiltonian  $\mathcal{H}(\gamma_1, \dots, \gamma_N)$ :

$$\begin{aligned} \mathcal{H}(\gamma_1, \dots, \gamma_N) \simeq & \sum_i u_1(\gamma_i) + \sum_{i < j} u_2(\gamma_i, \gamma_j) \\ & + \sum_{i < j < k} u_3(\gamma_i, \gamma_j, \gamma_k) + \dots \end{aligned} \quad (23)$$

The gauge invariance and translational invariance of the vacuum imply that the one-body term of the  $i$ th

pseudoparticle,  $u_1(\gamma_i)$ , is only a function of its size  $\rho_i$ . Hence, the function  $n(\rho_i) = \exp[-u_1(\gamma_i)]$  is called the (single-)instanton size distribution. The divergence of such a term in the semiclassical dilute gas limit gives rise to the ‘‘infrared catastrophe.’’ The terms  $u_2(\gamma_i, \gamma_j)$ ,  $u_3(\gamma_i, \gamma_j, \gamma_k)$ , ... describe multibody interactions, and depend in general also on the relative positions and color orientations of the pseudoparticles. With such a definition, and for  $\theta = 0$ , the partition function reads

$$\begin{aligned} Z_{\text{YM}} = & \sum_{N_+, N_-} \frac{1}{N_+! N_-!} \int \prod_i^N d\gamma_i \left( \prod_{i=1}^{N_+ + N_-} n(\rho_i) \right) \\ & \times e^{-\sum_{i < j} u_2(\gamma_i, \gamma_j) + \sum_{i < j < k} u_3(\gamma_i, \gamma_j, \gamma_k) + \dots} \end{aligned} \quad (24)$$

In the following, we present a computation of the single-instanton size distribution  $n(\rho)$ . The calculation of the many-body terms is conceptually analog and is referred to future work.

## B. Computing the instanton size distribution $n(\rho)$

In order to calculate  $n(\rho)$ , we have implemented the VMP method on the functional manifold spanned by individual instantons (and anti-instantons) defined in the singular gauge, which is a Landau gauge. The system of coordinates  $\{g_{\gamma_i, \mu}(x, \bar{\gamma})\}$  was obtained by numerically differentiating the instanton field (20) and (21) with respect to each of the eight collective coordinates:

$$\begin{aligned} g_{\rho, \mu}(x, \bar{\rho}, \bar{z}, \{\bar{\theta}_i\}) &= \frac{\tilde{A}_\mu(x; \bar{\rho} + \Delta\rho) - \tilde{A}_\mu(x; \bar{\rho} - \Delta\rho)}{2\Delta\rho}, \\ g_{z^\nu, \mu}(x, \bar{\rho}, \bar{z}, \{\bar{\theta}_i\}) &= \frac{\tilde{A}_\mu(x; \bar{z}^\nu + \Delta z^\nu) - \tilde{A}_\mu(x; \bar{z}^\nu - \Delta z^\nu)}{2\Delta z^\nu}, \\ & (\nu = 1, 2, 3, 4) \\ g_{\theta_i, \mu}(x, \bar{\rho}, \bar{z}, \{\bar{\theta}_i\}) &= \frac{\tilde{A}_\mu(x; \bar{\theta}_i + \Delta\theta) - \tilde{A}_\mu(x; \bar{\theta}_i - \Delta\theta)}{2\Delta\theta_i}, \\ & (i = 1, 2, 3), \end{aligned} \quad (25)$$

where  $\bar{\rho}$ ,  $\bar{z}^1$ ,  $\bar{z}^2$ ,  $\bar{z}^3$ ,  $\bar{z}^4$ ,  $\bar{\theta}_1$ ,  $\bar{\theta}_2$ ,  $\bar{\theta}_3$  define an arbitrary point on the manifold, whose choice will be specified below.

In the VMP method, the distribution of collective coordinates is obtained by projecting lattice field theory configurations, and solving the system of equations (8). We used three different ensembles of  $SU(2)$  Landau gauge-fixed lattice QCD configurations, generated using the Wilson action [32]:

- (i) an ensemble of 100 configurations generated on a  $16^4$  lattice at  $\beta = 2.3$  (corresponding to a lattice spacing  $a \simeq 0.17$  fm);
- (ii) an ensemble of 100 configurations generated on a  $24^4$  lattice at  $\beta = 2.4$  (corresponding to a lattice spacing  $a \simeq 0.12$  fm);

- (iii) an ensemble of 25 configurations generated on a  $32^4$  lattice at  $\beta = 2.5$  (corresponding to a lattice spacing  $a \approx 0.09$  fm).

The gauge-fixing procedure of the lattice configurations was based on an over-relaxation algorithm, described in detail in the original publication [32]. In general, such a minimization does not completely fix the gauge, allowing for the emergence of Gribov copies, which correspond to the local minima of the functional being minimized numerically. In particular, the gluon and ghost propagators evaluated this way have been shown to display a dependence on the choice of Gribov copies in the infrared region  $p < 0.5$ –1 GeV [32–34]. In the following, we shall assume that such a Gribov ambiguity does not significantly affect the results of our calculation.

In order to reduce the statistical uncertainty, we have projected each lattice configuration on ten different projection points on the manifold. The space-time coordinates of the projection points  $\bar{z}_1, \dots, \bar{z}_4$  and the color orientation coordinates  $\bar{\theta}_1, \bar{\theta}_2, \bar{\theta}_3$  were chosen randomly. On the other hand, the instanton size  $\bar{\rho}$  of the projection points was held fixed to five lattice spacings,  $\bar{\rho} = 5a$ . This choice was made in order to ensure that  $\bar{\rho}$  was always much larger than the lattice spacing  $a$ , yet much smaller than the size of the simulation box.

Treating results of the projection of the same lattice configuration on different points of the manifold as independent and uncorrelated measurements is justified as long as the typical average four-dimensional distance  $\bar{d}$  between two randomly picked projection points is much larger than the average instanton size  $\bar{\rho}$ . In particular, if  $N$  is the number of projection points and  $V$  is the volume of the box, the average distance between the projection points is

$\bar{d} \sim (N/V)^{1/4}$ . It is immediate to check that the condition  $\bar{d} \ll \bar{\rho} \approx 0.2$  fm is satisfied for all lattices considered.

Once the projection equations (11) were solved numerically for all lattice configurations and for all projection points, the probabilities for the collective coordinates  $\rho, z^\nu, \theta_1, \theta_2$ , and  $\theta_3$  were inferred from the corresponding frequency histograms. The distribution of the positions  $z$  and color orientation angles  $\theta_1, \theta_2, \theta_3$  are trivial, as a consequence of the gauge invariance and translational invariance of the vacuum. On the other hand, the probability distribution  $n(\rho)$  for the instanton size  $\rho$  was found to display nontrivial structure, as it is expected as a consequence of dimensional transmutation.

The instanton size distributions  $n(\rho)$  obtained from the three different ensembles of lattice configurations are shown in Fig. 2. Assuming a normal distribution, the statistical errors on such distributions can be estimated from the root of the number of points in each bin of the frequency histogram. This way, we find that the relative error on the calculated size distribution turns out to be of the order of 5%–15%. Within such a statistical error, the results are independent from the value of the lattice spacing  $a$ . The obtained distributions are peaked around  $\rho \approx 0.25$  fm and qualitatively agree with the results of other methods (see right panel of Fig. 2). On the other hand, we stress that the present results do not depend on any arbitrary parameter, and take into account the full quantum content of the lattice configurations.

It is instructive to compare the small instanton size tail of the  $n(\rho)$  distribution obtained nonperturbatively through the VMP method with the analytical one-loop formula obtained by 't Hooft [35],

$$n_{\text{one-loop}}(\rho) \propto \rho^{(11/3)N_c - 5}. \quad (26)$$

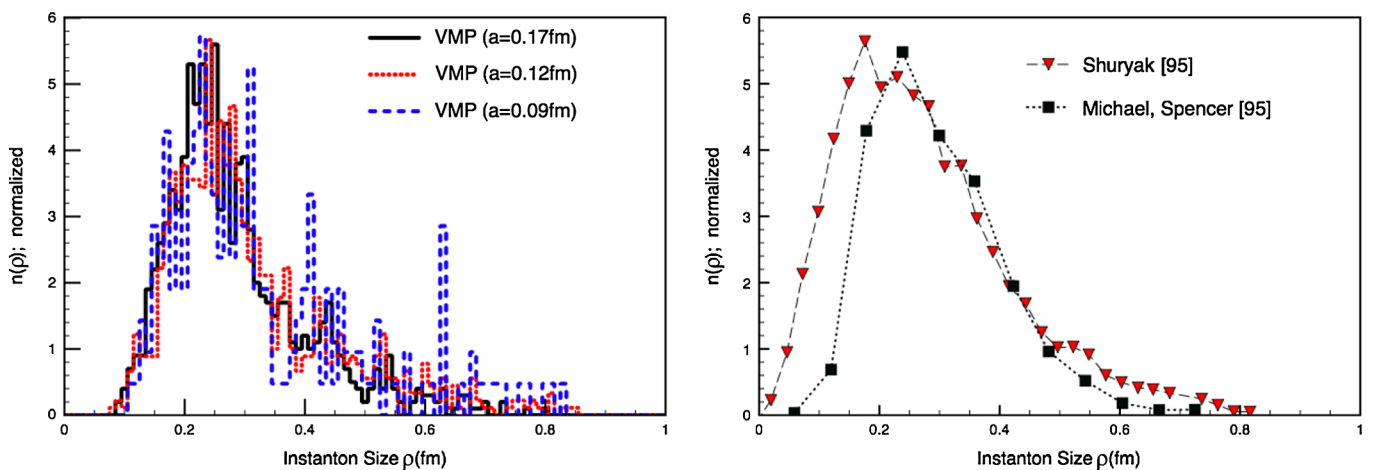


FIG. 2 (color online). Left panel: Instanton size distribution  $n(\rho)$  obtained with the VMP technique, from three different sets of *gauge-fixed* configurations. The results have been obtained with  $\bar{\rho} = 5a$ . Right panel: Results for pure gauge  $SU(2)$  obtained by Michael and . Spencer from lattice simulations using the cooling algorithm (squares) [39] and by Shuryak from interacting instanton liquid model simulations (triangles) [40].

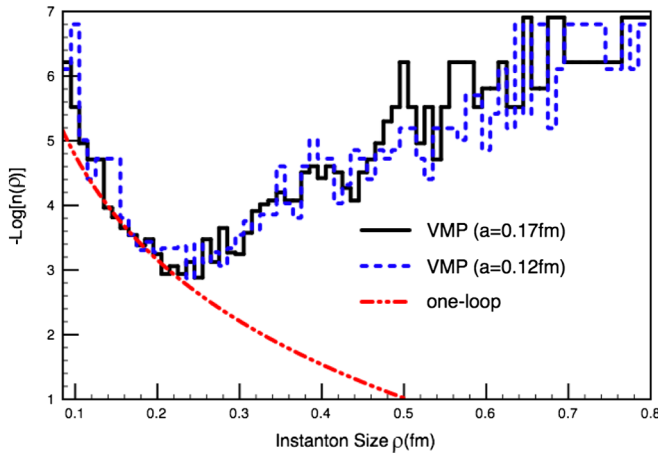


FIG. 3 (color online). Logarithm of the instanton size distribution  $n(\rho)$ , obtained with the VMP technique from two different sets of *gauge-fixed* configurations. The results are compared with the exact one-loop calculation obtained by 't Hooft [35]. The VMP results are in agreement with the one-loop calculation, in the small-sized instantons range  $0.1 \text{ fm} \lesssim \rho \lesssim 0.2 \text{ fm}$ . The VMP results for very small-sized instantons ( $\rho \lesssim 0.1 \text{ fm}$ ) is affected by lattice discretization errors.

In Fig. 3 we show that our results are in quantitative agreement with the leading-order perturbative prediction in the range  $0.1 \text{ fm} \lesssim \rho \lesssim 0.2 \text{ fm}$ . The VMP results for very small-sized instantons ( $\rho \lesssim 0.1 \text{ fm}$ ) are affected by lattice discretization errors, while the perturbative calculation is not reliable for large instanton sizes,  $\rho \gtrsim 1/\Lambda_{SU(2)}$ . Such a comparison shows that the suppression of the large-sized instantons is a purely nonperturbative effect.

It is also interesting to compare our fully nonperturbative result, with the variational estimate of the instanton size distribution obtained by Diakonov and collaborators [5,36]:

$$n_{\text{var}}(\rho) = n_{\text{one-loop}}(\rho) e^{-((11/6)N_c - 2)(\rho^2/\langle \rho^2 \rangle)}. \quad (27)$$

Note that such a variational ansatz assumes an exponential suppression of large-size instantons. In order to test such an assumption, we performed a fit of (27) on our VMP data, obtained using the  $a = 0.12 \text{ fm}$  lattice. Such a fit was restricted to the range  $\rho \in [a, 1 \text{ fm}]$  in order to avoid the bias from discretization errors. The best fit is shown in Fig. 4, which corresponds to choosing

$$\langle \rho^2 \rangle_{\text{fit}} = 0.083(3) \text{ fm}^2. \quad (28)$$

This parameter is very close to the numerical value of the second moment evaluated from the  $a = 0.12 \text{ fm}$  VMP data:

$$\langle \rho^2 \rangle_{\text{VMP}(a=0.12 \text{ fm})} = 0.12(3) \text{ fm}^2. \quad (29)$$

In addition, also the first moment of the fitted curve is compatible with the VMP results:

$$\langle \rho \rangle_{\text{fit}} = 0.27(1) \text{ fm} \quad (30)$$

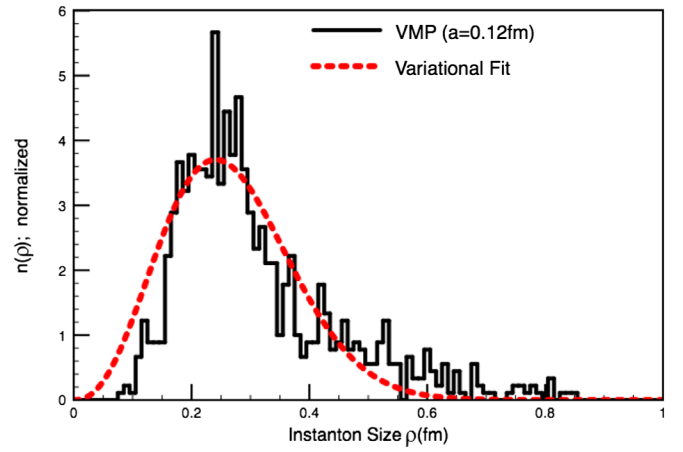


FIG. 4 (color online). Solid line: Instanton size distribution  $n(\rho)$  obtained with the VMP technique, from *gauge-fixed* configurations with  $a = 0.12 \text{ fm}$ ; dashed line: result of the fit of the VMP data in the range  $\rho \in [a, 1 \text{ fm}]$ , with the variational estimate  $n_{\text{var}}(\rho)$  in Eq. (27).

$$\langle \rho \rangle_{\text{VMP}(a=0.12 \text{ fm})} = 0.31(4) \text{ fm}. \quad (31)$$

We conclude that variational estimates of the instanton size distribution can be considered realistic.

We conclude this part by commenting on the fact that, although the total number of pseudoparticles which are present in a given lattice configuration is neither fixed nor known, the one-body instanton density has been calculated by projecting onto a single-instanton manifold. This is made possible by the fact that the projection functions for the single-instanton manifold are peaked around the projection point. Whatever the number of instantons in the box, the projection method will only characterize the size of the pseudoparticle nearest to the projection point. Similarly, if the vacuum ensemble is sufficiently dilute, the calculation of the two-body terms may be performed by projecting onto a two-pseudoparticle manifold, as was done in Ref. [10]. Clearly, this way, it is not possible to compute the normalization of the different terms in the effective Hamiltonian (e.g. the total number of instantons and anti-instantons). On the other hand, these normalization constants can be evaluated *a posteriori*, by minimizing the free energy of the statistical vacuum model—see e.g. Ref. [37].

### C. Testing the accuracy of the VMP calculation of the instanton size

In this section we present a study of the accuracy of our VMP calculation of the instanton size distribution based on an instanton model. We generated 1000 configurations of an ensemble of configurations constructed by superimposing the fields of 20 instantons and 20 anti-instantons in a box of volume  $V = (2.7 \text{ fm})^4$ . The positions and color orientations of the pseudoparticles were randomly chosen, while the size of the pseudoparticles was sampled from a Gaussian distribution:

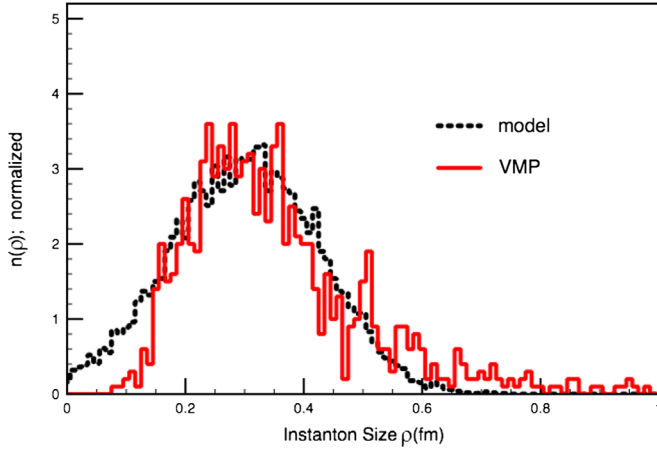


FIG. 5 (color online). Comparison between the distribution used to generate an instanton ensemble with density  $n \simeq 0.75 \text{ (fm}^{-4}\text{)}$  and the distribution obtained using the VMP approach from the corresponding lattice configurations.

$$n_{\text{model}}(\rho) \propto \exp\left[-\frac{(\rho - \rho_0)^2}{2\sigma^2}\right], \quad (0 \text{ fm} \leq \rho \leq 1 \text{ fm}), \quad (32)$$

with  $\rho_0 = 0.3 \text{ fm}$  and  $\sigma = 0.13 \text{ fm}$ . The field configurations were discretized on a lattice of spacing  $a = 0.17 \text{ fm}$ . The VMP procedure outlined above was applied to such an ensemble of instanton-model lattice configurations in order to compute instanton size distribution  $n(\rho)$ . In Fig. 5 we compare the distribution  $n(\rho)$  calculated through the VMP method and the exact  $n_{\text{model}}(\rho)$  which was used to generate the instantons ensemble. We see that the VMP approach allows one to very accurately reconstruct the correct instanton size distribution for all values of the instanton size larger than about a lattice spacing.

#### IV. CONCLUSIONS

In this work we have presented the first application of the recently developed VMP method to a gauge theory. We have used such a method to perform a nonperturbative calculation of the instanton size distribution in  $SU(2)$  gluon dynamics. Our results are in good agreement with other lattice calculations for all  $\rho$ , and with the one-loop perturbative estimate, in the small instanton size regime. The

VMP calculations of the many-body terms of the effective Hamiltonian of the instanton vacuum models are conceptually analog to the one presented here. For example, in order to compute the instanton-instanton two-body interaction  $u_2(\gamma_i, \gamma_k)$ , one would need to project onto the manifold spanned by the collective coordinates of two pseudoparticles. Such a calculation was performed in [10] in the case of a quantum-mechanical toy model and its extension to gauge theories does not raise conceptual difficulties.

It should be emphasized that, in the present calculation, the fluctuations around the instanton field are not just filtered away, as in the cooling or eigenvalue filtering algorithms. Instead, they are systematically integrated out. As a result, the calculation is entirely self-consistent and does not depend on any arbitrary external parameter. Recently, Perez and co-workers have proposed a so-called adjoint filtering method based on Dirac quasizero modes in the adjoint representation [38], which does not rely on additional parameters. This method has been used to study the dynamics of smooth single-instanton configurations "heated" by Monte Carlo updating steps. The present VMP method discussed in this paper could be used in principle to perform the same task. On the other hand, the VMP approach can be applied also to vacuum field configurations which are not solutions of the equation of motion. For example, it may be used to guide the development of vacuum models based on dyonic degrees of freedom.

#### ACKNOWLEDGMENTS

P. F. is a member of the Interdisciplinary Laboratory for Computational Science (LISC), a joint venture of Trento University and FBK. R. M. is presently supported by the Research Executive Agency (REA) of the European Union under Grant Agreement No. PITN-GA-2009-238353 (ITN STRONGnet). The VMP approach was developed in collaboration with L. Scorzato, who we gratefully acknowledge. We are also indebted to F. Di Renzo for making observations which triggered our work, with F. Pederiva for important discussions, and with A. Sternbeck for providing us with gauge-fixed  $SU(2)$  lattice configurations. Finally, we thank D. Diakonov for suggesting a comparison with variational estimates of the instanton density.

- 
- [1] T. Schaefer and E. V. Shuryak, *Rev. Mod. Phys.* **70**, 323 (1998).  
 [2] G. Ripka, *Dual superconductor Models of Color Confinement*, Lecture Notes in Physics, Vol. 639 (Springer-Verlag, Berlin, Heidelberg, 2004).  
 [3] R. Bertle, J. Greensite, and S. Olejnik, *Quark Confinement and the Hadron Spectrum IV: Proceedings*, edited by

- Wolfgang Lucha and Khin Maung Maung (World Scientific, Singapore, 2002).  
 [4] F. Lenz, J. W. Negele, and M. Thies, *Ann. Phys. (N.Y.)* **323**, 1536 (2008).  
 [5] D. Diakonov and V. Yu Petrov, *Nucl. Phys.* **B245**, 259 (1984).  
 [6] P. Faccioli and T. DeGrand, *Phys. Rev. Lett.* **91**, 182001 (2003)

- [7] C. Gattringer, *Phys. Rev. Lett.* **88**, 221601 (2002).
- [8] A. Di Giacomo, *AIP Conf. Proc.* **964**, 348 (2007).
- [9] J. M. Cornwall, *Proc. Sci.*, QCD-TNT09 (2009) 007.
- [10] R. Millo, P. Faccioli, and L. Scorzato, *Phys. Rev. D* **81**, 074019 (2010).
- [11] C. T. H. Davies *et al.*, *Phys. Rev. D* **37**, 1581 (1988).
- [12] L. Giusti, M. L. Paciello, C. Parrinello, S. Petrarca, and B. Taglienti, *Int. J. Mod. Phys. A* **16**, 3487 (2001).
- [13] A. R. Leach, *Molecular Modeling: Principles and Applications* (Pearson Education Limited, Harlow, 2001), 2nd ed.
- [14] D. Diakonov, [arXiv:hep-ph/9602375v1](https://arxiv.org/abs/hep-ph/9602375v1).
- [15] M. Cristoforetti, P. Faccioli, J. W. Negele, and M. Traini, *Phys. Rev. D* **75**, 034008 (2007).
- [16] M. Cristoforetti, P. Faccioli, and M. Traini, *Phys. Rev. D* **75**, 054024 (2007).
- [17] P. Faccioli, *Phys. Rev. D* **65**, 094014 (2002).
- [18] T. Schäfer and E. V. Shuryak, *Phys. Rev. Lett.* **75**, 1707 (1995).
- [19] H. Forkel, *Phys. Rev. D* **64**, 0244015 (2001); H. Forkel, *Phys. Rev. D* **71**, 054008 (2005).
- [20] M. C. Tichy and P. Faccioli, *Eur. Phys. J. C* **63**, 423 (2009).
- [21] V. Mathieu, N. Kochelev, and V. Vento, *Int. J. Mod. Phys. E* **18**, 1 (2009).
- [22] P. Faccioli, A. Schwenk, and E. V. Shuryak, *Phys. Lett. B* **549**, 93 (2002).
- [23] P. Faccioli, *Phys. Rev. C* **69**, 065211 (2004).
- [24] P. Faccioli, A. Schwenk, and E. V. Shuryak, *Phys. Rev. D* **67**, 113009 (2003).
- [25] P. Faccioli, D. Guadagnoli, and S. Simula, *Phys. Rev. D* **70**, 074017 (2004).
- [26] N. I. Kochelev and V. Vento, *Phys. Rev. Lett.* **87**, 111601 (2001).
- [27] M. Cristoforetti, P. Faccioli, E. V. Shuryak, and M. Traini, *Phys. Rev. D* **70**, 054016 (2004).
- [28] M. Cristoforetti, P. Faccioli, G. Ripka, and M. Traini, *Phys. Rev. D* **71**, 114010 (2005).
- [29] F. Lenz, J. W. Negele, and M. Thies, *Phys. Rev. D* **69**, 074009 (2004).
- [30] E. V. Shuryak, *Nucl. Phys.* **B203**, 93 (1982).
- [31] M. Chu, J. Grandy, S. Huang, and J. W. Negele, *Phys. Rev. D* **49**, 6039 (1994).
- [32] A. Sternbeck *et al.*, *Proc. Sci.*, LAT2007 (2007) 340.
- [33] A. Sternbeck *et al.*, *Phys. Rev. D* **72**, 014507 (2005).
- [34] I. L. Bogolubsky *et al.*, *Proc. Sci.*, LAT2009 (2009) 237.
- [35] G. 't Hooft, *Phys. Rev. D* **14**, 3432 (1976).
- [36] D. Diakonov, M. V. Poliakov, and C. Weiss, *Nucl. Phys.* **B461**, 539 (1996).
- [37] T. Schäfer and E. V. Shuryak, *Phys. Rev. D* **53**, 6522 (1996).
- [38] M. G. Perez, A. González-Arroyo, and A. Sastre, *J. High Energy Phys.* **07** (2011) 034.
- [39] C. Michael and P. S. Spencer, *Phys. Rev. D* **52**, 4691 (1995).
- [40] E. V. Shuryak, *Phys. Rev. D* **52**, 5370 (1995).